

Tidal Evolution of Rubble Piles

Peter Goldreich^{1,2} and Re'em Sari^{2,3}

¹*Institute for Advanced Study, Princeton, NJ*

²*Caltech 130-33, Pasadena, CA 91125*

³*Racah Institute of Physics, Hebrew University, Jerusalem 91904, Israel.*

ABSTRACT

Many small bodies in the solar system are believed to be rubble piles, a collection of smaller elements separated by voids. We propose a model for the structure of a self-gravitating rubble pile. Static friction prevents its elements from sliding relative to each other. Stresses are concentrated around points of contact between individual elements. The effective dimensionless rigidity, $\tilde{\mu}_{rubble}$, is related to that of a monolithic body of similar composition and size, $\tilde{\mu}$ by $\tilde{\mu}_{rubble} \sim \tilde{\mu}^{1/2} \epsilon_Y^{-1/2}$, where $\epsilon_Y \sim 10^{-2}$ is the yield strain. This represents a reduction in effective rigidity below the maximum radius, $R_{max} \sim [\mu \epsilon_Y / (G \rho^2)]^{1/2} \sim 10^3$ km, at which a rubble pile can exist. Densities derived for binary near-Earth asteroids imply that they are rubble piles. As a consequence, their tidal evolution proceeds 10^3 to 10^4 times faster than it would if they were monoliths. This accounts for both the sizes of their semimajor axes and their small orbital eccentricities. We show that our model for the rigidity of rubble piles is compatible with laboratory experiment in sand.

Subject headings: asteroids

1. Introduction

Rubble piles are bodies composed of smaller elements separated by voids. There is compelling evidence that at least some small solar system bodies are rubble piles bound by gravity. Their telltale signature is a mean density below that of their constituent elements. Examples include: four icy satellites of Saturn, the coorbitals, Janus and Epimetheus, and the F-ring shepherds, Prometheus and Pandora (Jacobson & French 2004; Porco et al. 2007), the rocky main belt asteroids, C-type 253 Mathilde (Veveřka et al. 1997; Yeomans et al. 1997) and M-type 22 Kalliope (Margot & Brown 2003), and the binary near-Earth asteroid 1999 KW4 (Ostro et al. 2006). The largest of these bodies, Janus and Kalliope, have dimensions

of order 100 km. It is unclear whether larger rubble piles exist or whether all smaller bodies are rubble piles.

Intuitively we expect a rubble pile to be weaker than a monolithic body of the same composition. Thus tidal dissipation at a rate that is more rapid than typical for a monolith is considered evidence for a rubble pile (Margot & Brown 2003). The orbits of binary near-Earth asteroids are prime examples; the sizes of their semimajor axes and their low orbital eccentricities suggest that they are evolving tidally at rates between 10^3 and 10^4 times faster than estimates for monolithic bodies of similar size would predict (Walsh & Richardson 2006a). In what follows, we provide a theoretical basis for estimating tidal dissipation rates in rubble piles and show that it can account for this large speedup of tidal evolution.

The plan of our paper is as follows. In §2, we formulate a quantitative theory for the effective rigidity of a self-gravitating rubble pile and demonstrate that it is due to voids rather than cracks. Limits on the sizes of rubble piles are derived in §3. In §4, we apply our theory to the tidal evolution of binary near-Earth asteroids.

2. Effective Elastic Modulus Of A Rubble Pile

We begin by reviewing the tidal response of a uniform body of density ρ , rigidity μ , and radius R . As is customary, we define the dimensionless rigidity by $\tilde{\mu}$;

$$\tilde{\mu} \equiv \frac{19\mu}{2g\rho R}. \quad (1)$$

Next we show that $\tilde{\mu}$ is the ratio of the fluid strain to the elastic strain.¹

We assume that the tidal force, f , is weak in comparison to the cohesive force of the body's self gravity, gM , where $g \sim G\rho R$. If the body were fluid, $\mu = 0$, it would suffer a strain

$$\epsilon_g \sim \frac{f}{g\rho R^3}, \quad (2)$$

whereas if it were elastic but lacked self-gravity, $g = 0$, the strain would be

$$\epsilon_\mu \sim \frac{f}{\mu R^2}. \quad (3)$$

To order of magnitude, the ratio between expressions (2) and (3) reproduces $\tilde{\mu}$ given by equation (1).

¹Arguments in this section are order of magnitude only.

How does the tidal response of a rubble pile differ from that of a monolith? To answer this question, we investigate some simple models.

2.1. cracks do not matter

Normal stresses are seamlessly transmitted across cracks, so a body’s response to weak tides is unaffected by cracks. Consider a body of radius R composed of cubical elements whose sides have length $r \ll R$. The ratio of the weight of a single cube, $gM(r/R)^3$, to the divergence of tidal stress acting on its volume, $f(r/R)^3$, is just gM/f . Thus a coefficient of static friction larger than f/gM would suffice to prevent the cubes from slipping relative to each other. Coefficients of static friction for rocks and dry ice are of order unity, and $f/gM \sim (R/a)^3$ for an equal mass binary with semi-major axis a .

2.2. voids are key

2.2.1. uniform spheres

Next we consider a body of radius R composed of identical spheres of radius $r \ll R$. Its mean density $\bar{\rho} \approx 0.7\rho$. A typical cross section cuts $(R/r)^2$ small spheres each of which transmits forces $F(r/R)^2$ to its neighbors, where $F \sim gM + f$ includes both tidal forces and self gravity. In so doing, each small sphere undergoes a linear distortion δx and forms contact surfaces with its neighbors of area $\delta x r$. Within $(\delta x r)^{1/2}$ of each contact, the strain is of order $(\delta x/r)^{1/2}$ so

$$F \left(\frac{r}{R}\right)^2 \sim \mu r^{1/2} \delta x^{3/2}. \quad (4)$$

The average strain is just $\delta x/r$, where from equation (4)

$$\frac{\delta x}{r} \sim \left(\frac{F}{\mu R^2}\right)^{2/3}. \quad (5)$$

Most of this strain is due to the body’s self-gravity. To isolate the tidal strain, we expand $F^{2/3}$ in equation (5) around $F \sim gM$ to obtain

$$\epsilon \sim \frac{f}{\mu R^2} \left(\frac{\mu}{g\rho R}\right)^{1/3}. \quad (6)$$

Thus the effective dimensionless tidal rigidity of a body composed of identical spheres is

$$\tilde{\mu}_{spheres} \sim \left(\frac{\mu}{g\rho R}\right)^{1/3} \sim \tilde{\mu}^{2/3}. \quad (7)$$

This result is equivalent to that originally established by Duffy & Mindlin (1957).

2.2.2. irregular fragments

Natural rubble piles are likely to be composed of irregularly shaped elements whose surfaces have local radii of curvature, \hat{r} , that are much smaller than the elements' sizes, r . Compared to rubble piles composed of spheres, contact areas would be reduced, stress concentrations increased, and the effective rigidity lowered. A simple modification of the derivation given in 2.2.1 suffices to evaluate the effective rigidity of a rubble pile, $\tilde{\mu}_{rubble}$. Each element still transmits its share of the total force. However, \hat{r} must replace r on the right hand side of equation (4). Thus now

$$\frac{\delta x}{r} \sim \left(\frac{F}{\mu R^2} \right)^{2/3} \left(\frac{r}{\hat{r}} \right)^{1/3}. \quad (8)$$

Continuing as before, we find that the average strain across the rubble pile is increased by the factor $(r/\hat{r})^{1/3}$ with the consequence that the effective rigidity now reads

$$\tilde{\mu}_{rubble} \sim \tilde{\mu}_{spheres} \left(\frac{\hat{r}}{r} \right)^{1/3} \sim \tilde{\mu}^{2/3} \left(\frac{\hat{r}}{r} \right)^{1/3}. \quad (9)$$

The sharper the contact points, the softer the rubble pile, up to a limit at which the stress near the contact surfaces reaches the material's yield stress σ_Y , or yield strain $\epsilon_Y = \sigma_Y/\mu$. This limit is met at

$$\frac{\hat{r}}{r} \sim \frac{1}{(\tilde{\mu}\epsilon_Y^3)^{1/2}} \quad (10)$$

Sharper contact points than allowed by equation (10) would be dulled by material flow or failure. Therefore,

$$\tilde{\mu}_{rubble} \gtrsim \left(\frac{\tilde{\mu}}{\epsilon_Y} \right)^{1/2}. \quad (11)$$

Experimentally it is generally found that the effective rigidity of a granular material scales in direct proportion to the square root of the confining pressure. Goddard (1990) provides an explanation for this scaling which is similar to ours.

Equations (7) and (9) demonstrate that the effective rigidity of a rubble pile is smaller than that of a monolithic body of the same size. The reduction in rigidity is independent of the sizes of the elements into which the body is divided. It arises from the concentration of stresses due to the presence of voids.

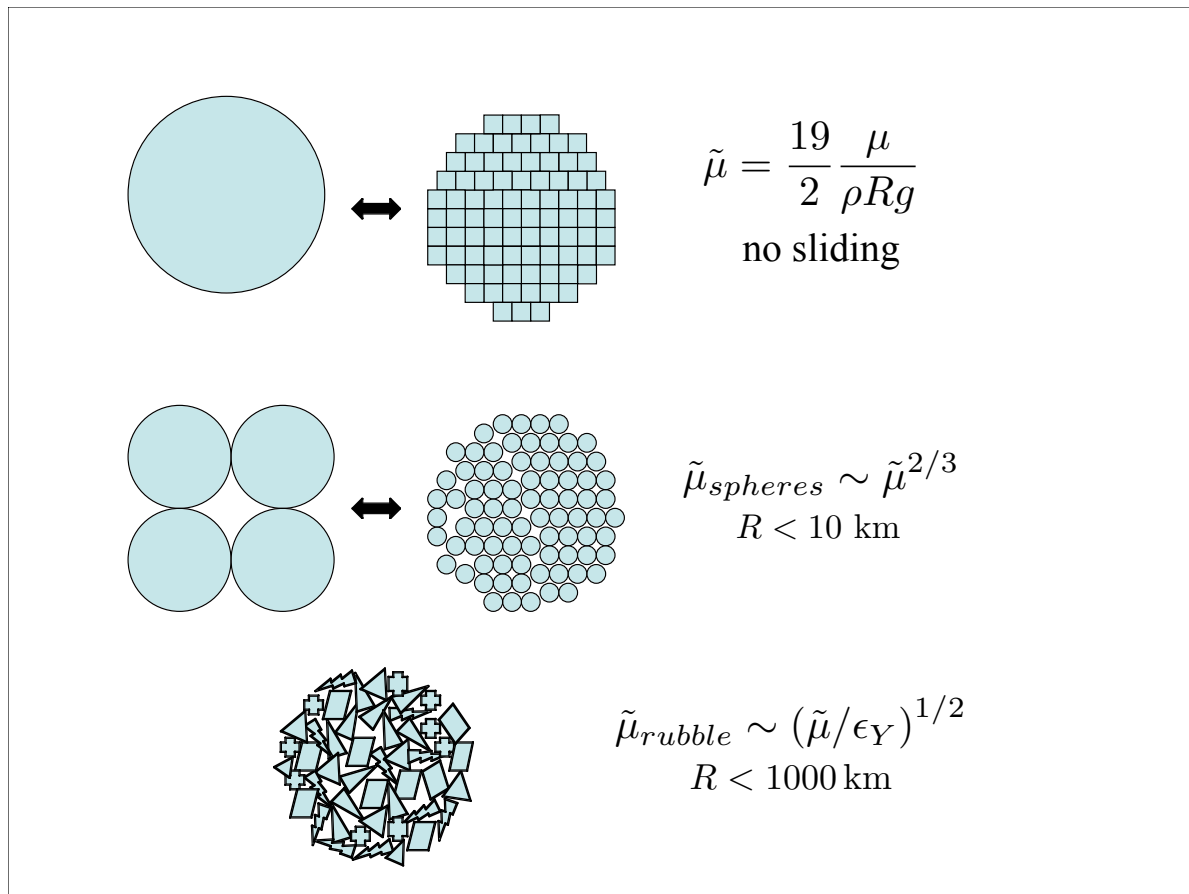


Fig. 1.— Three simple models of fragmented bodies. Upper row depicts a body composed of cubical elements. There are no voids. Static friction prevents the elements from sliding relative to each other. Its effective rigidity is identical to that of a monolith. Middle row shows a body composed of spherical elements. Voids are present. Stresses concentrate near contacts between elements. The effective rigidity is smaller than that of a monolith and is independent of the sizes of the elements. Such an idealized configuration requires the spheres to be sufficiently smooth. If made of rock or ice, its radius could not be larger than about 10 km. Bottom row illustrates a more realistic rubble pile composed of irregular elements. Sharper contact points increase stress concentration more than for a body composed of spherical elements. Accordingly, its effective rigidity is further decreased. Radii of rubble piles composed of rock or ice cannot be larger than about 1000 km.

2.3. energy considerations

We re-derive equation (9) based on energy considerations. Strains of order $(\delta x/\hat{r})^{1/2}$ are attained within a distance $(\delta x \hat{r})^{1/2}$ of the contacts between individual elements. Thus the elastic energy stored within the rubble pile satisfies

$$\delta E \sim \mu(\delta x)^{5/2}\hat{r}^{1/2} \left(\frac{R}{r}\right)^3. \quad (12)$$

We can also express δE in terms of the effective dimensionless rigidity, $\tilde{\mu}_{rubble}$ and the average strain in the rubble pile, $\delta x/r$ as

$$\delta E \sim \tilde{\mu}_{rubble} g \rho R \left(\frac{\delta x}{r}\right)^2 R^3. \quad (13)$$

Equating the expressions for δE given in equations (12) and (13), we arrive at

$$\tilde{\mu}_{rubble} \sim \tilde{\mu} \frac{\delta x^{1/2} \hat{r}^{1/2}}{r}. \quad (14)$$

Finally, by using equation (8) to eliminate δx , we recover equation (9).

3. Critical Sizes For Rubble Piles

3.1. mechanical limits

At

$$R = R_* \sim \left(\frac{\mu \epsilon_Y^3}{\rho^2 G}\right)^{1/2}, \quad (15)$$

which corresponds to $\tilde{\mu} \sim \epsilon_Y^{-3}$, $\tilde{\mu}_{rubble} \sim \tilde{\mu}_{spheres} \sim \epsilon_Y^{-2}$ and $\hat{r}/r \sim 1$. For nominal values of $\mu_{rock} \approx 5 \times 10^{11}$ dyne cm⁻², $\mu_{ice} \approx 3 \times 10^{10}$ dyne cm⁻², $\epsilon_Y \sim 10^{-2}$, $R_* \sim 10$ km for rubble piles composed of either rock or ice. Moreover, $\tilde{\mu}_{rubble} \sim 10^4$ as compared to $\tilde{\mu} \sim 10^6$ for a monolith of radius R_* . At

$$R_{max} = \left(\frac{\mu \epsilon_Y}{\rho^2 G}\right)^{1/2}, \quad (16)$$

which corresponds to $\tilde{\mu} \sim \epsilon_Y^{-1}$ and $\hat{r}/r \sim \epsilon_Y^{-2}$, the contact areas are comparable to the surface areas of individual elements so $\tilde{\mu}_{rubble} \sim \tilde{\mu}$. With nominal parameters, $R_{max} \sim 10^3$ km and $\tilde{\mu}_{rubble} \sim \tilde{\mu} \sim 10^2$.

A body with $R < R_*$ would avoid elastic failure if it were composed of identical spheres. For $R > R_*$, elastic failure would occur at points of contact among spheres. More generally,

we would expect the voids in rubble piles to occupy a decreasing fraction of the volume with increasing R up to $R = R_{max}$. At R_{max} , the average interior pressure $g\rho R_{max} \sim \sigma_Y$, so voids could only exist near the surface.

3.2. thermal limits

Rubble piles should be more common among smaller bodies because they cool more rapidly than larger ones and therefore are less likely to have been melted. Thermal diffusivities of rock and ice are of order $10^{-2} \text{ cm}^2 \text{ s}^{-1}$, which implies

$$t_{cool} \sim 3 \times 10^{10} \left(\frac{R}{10^3 \text{ km}} \right)^2 \text{ y}. \quad (17)$$

Even bodies as small as $R_* \sim 10 \text{ km}$ might have been melted if they formed early and were endowed with short lived radioactive nuclides. On the other hand, bodies as large as $R_{max} \sim 3 \times 10^2 \text{ km}$ which were fragmented by collisions after the short lived radioactive nuclides had decayed could have avoided melting.

4. Implications For Tidal Evolution

Tides play crucial role in orbital and spin evolution of binaries. Here we focus on the evolution after the secondary’s spin has become synchronous with the mean orbital angular velocity while the primary’s spin remains much faster. In this case, tides raised on the primary cause both the semimajor axis, a , and the orbital eccentricity, e , to grow while those raised on the secondary have negligible effect on the semimajor axis and cause the eccentricity to decay (Goldreich 1963; Goldreich & Soter 1966). Relevant expressions for $e \ll 1$ are:

$$\frac{1}{a} \frac{da}{dt} = 3 \frac{k_p}{Q_p} \frac{M_s}{M_p} \left(\frac{R_p}{a} \right)^5 n \quad (18)$$

and

$$\frac{1}{e} \frac{de}{dt} = \frac{57}{8} \frac{k_p}{Q_p} \frac{M_s}{M_p} \left(\frac{R_p}{a} \right)^5 n, \quad (19)$$

for tides raised on the primary, and

$$\frac{1}{e} \frac{de}{dt} = -\frac{21}{2} \frac{k_s}{Q_s} \frac{M_p}{M_s} \left(\frac{R_s}{a} \right)^5 n. \quad (20)$$

for tides raised on the secondary²

Tidal evolution rates depend on two parameters, k and Q . The estimation of k for monoliths involves little uncertainty. For a body of uniform density,

$$k = \frac{1.5}{1 + \tilde{\mu}}. \quad (21)$$

The estimation of Q is more uncertain. Available evidence suggests that $Q \sim 10^2$ for monolithic bodies (Goldreich & Soter 1966).

4.1. Semimajor axis evolution in binary rubble piles

Semimajor axis evolution is driven by the transfer of angular momentum from the spin of the primary to the orbit. Below, we estimate timescales for the semimajor axes of some well observed binary NEAs to have evolved from much smaller initial values to their current ones. Integrating equation (18), we obtain

$$T = \frac{2}{39} \frac{Q_p}{k_p} \frac{M_p}{M_s} \left(\frac{a}{R_p} \right)^5 \frac{1}{n} \quad (22)$$

We compare timescales for models in which the bodies are assumed to be monolithic solids, fluids, and rubble piles. We set $Q = 100$ in each case.

As the entries in table 1 demonstrate, the timescale for semimajor axis evolution is measured in Gyrs for monoliths, years for fluids, and Myrs for rubble piles. Only the latter is consistent with estimates of 10 Myr for the dynamical life time of NEAs (Gladman et al. 2000). Since it is plausible that the stress concentration in rubble piles results in $Q < 100$, the ages we estimate for rubble piles should be viewed as upper limits.

4.2. Comparison with experiments in sand

The effective rigidity of our model rubble pile, μ_{rubble} , is proportional to the square root of the confining pressure and independent of the size of the individual elements. Laboratory

²Subscripts p and s denote primary and secondary. We adopt standard notations for tidal Love number, k , and quality factor, Q (Murray & Dermott 2000). Q^{-1} is a stand-in for $\sin 2\delta$, where δ is the tidal phase lag.

measurements of the shear velocity, $c_s = \sqrt{\mu/\rho}$, in sand as a function of pressure provide a useful calibration. The data on $c_s(p)$ plotted in figure 1 of Goddard (1990) are replotted in our figure 2. On the figure’s upper boundary we display the radius of an asteroid whose average internal pressure

$$P = (4\pi/15)G\rho^2 R^2 \cong 2.2 \times 10^3 \left(\frac{R}{1 \text{ km}} \right)^2 \text{ dyne cm}^{-2} \quad (23)$$

with $\rho \cong 2 \text{ g cm}^{-3}$ corresponds to that given on the lower boundary. The range of pressures covered in the experiments on sand correspond to those inside asteroids with radii from 10-40 km. The right-hand boundary of the figure shows the effective rigidity corresponding to the shear velocity. It is well-fit by the solid line which is derived from our expression for effective rigidity with $\epsilon_Y \cong 0.17$. This should not be taken as evidence that the yield strain of sand is 0.17 since our formula is only accurate to order of magnitude. However, it does suggest that the ages we estimate in table 1 may be a factor of a few too large. The dashed line indicates the higher effective rigidity of a body composed of uniform quartz spheres.

Next we compare data on the rigidity of sand with that on the effective rigidity of NEAs. To do so, we assume that the semimajor axes of binary NEAs have evolved from much smaller initial values over $\sim 1 \text{ Myr}$ with a tidal $Q = 100$. Then we use equations (1), (18), and (21) to evaluate the effective tidal rigidity of the primary for each of the binaries in table 1. These rigidities are plotted as x’s on figure 2. Although the scatter is large, probably dominated by our assumption of a uniform age, the data fit nicely on the extrapolation to low pressure of the data from the experiments on sand.

4.3. rates of eccentricity evolution in binary rubble piles

Binary near-Earth asteroids are thought to form by Yorp³ spin up and/or tidal disruption and consequently be rubble piles (Walsh & Richardson 2006b). Most have nearly circular orbits from which Walsh & Richardson (2006a) argue that tidal damping of their orbital eccentricities proceeds 3 to 4 orders of magnitude faster than would be expected for binary monoliths of comparable size. A significant fraction of this increase must be due to the reduced rigidity of a rubble pile as compared to a monolith since Q cannot be smaller than unity.

³Yorp spin up has been measured for near-Earth asteroid 2000 PH5 (Lowry et al. 2007; Taylor et al. 2007).

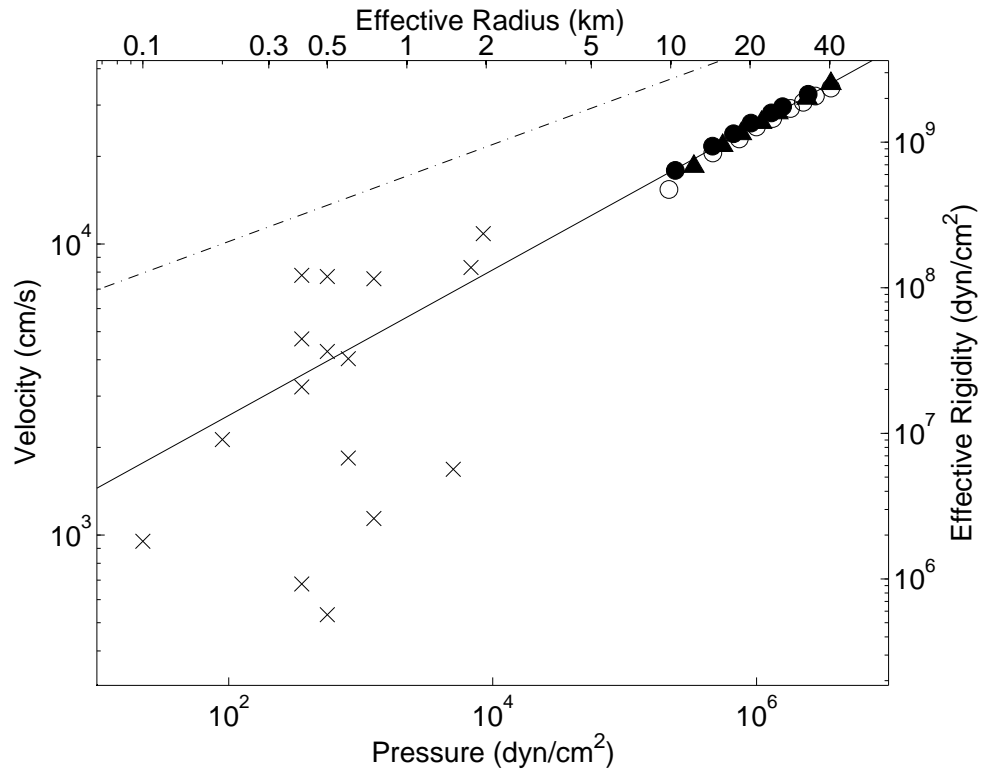


Fig. 2.— Comparison of our model for the effective rigidity of rubble piles with that from experiments on sand taken from Goddard (1990). Shear wave velocity as a function of pressure in saturated, dry, and drained Ottawa sands is shown by open circles, solid circles, and triangles, respectively. Effective rigidities of NEAs, inferred by assuming binary ages of 1Myr and $Q = 100$, are plotted against the primary diameter and marked by x's.

For rocky bodies, scaling from the tidal Love number of the Moon, $k_{Moon} \approx 0.03$,

$$\tilde{\mu} \approx 1.5 \times 10^8 \left(\frac{\text{km}}{R} \right)^2, \quad (24)$$

which corresponds to $\mu \approx 5 \times 10^{11} \text{ dyne cm}^{-2}$. Thus from equation (11) with $\epsilon_Y = 10^{-2}$, we obtain

$$\frac{\tilde{\mu}}{\tilde{\mu}_{rubble}} \lesssim (\tilde{\mu}\epsilon_Y)^{1/2} \approx 10^3 \frac{\text{km}}{R}. \quad (25)$$

Since typical secondaries among near earth asteroid binaries have radii of a few tenths of a kilometer, much if not all of the increase in the inferred rates of eccentricity damping might be due to an increase of k . However, it would not be surprising if a contribution came from a reduction of Q .

We note that close encounters with Earth or other planets might reset the eccentricities of binary NEAs on timescales comparable to those at which they evolve under tides. This issue deserves investigation.

4.3.1. conditions for eccentricity damping in binary asteroids

If both primary and secondary were strength rather than gravity dominated ($\tilde{\mu} \gg 1$), then the ratio of the rates of eccentricity excitation and damping would be

$$\mathcal{R} = \frac{19}{28} \left(\frac{\rho_s}{\rho_p} \right)^2 \frac{R_s \tilde{\mu}_s Q_s}{R_p \tilde{\mu}_p Q_p}. \quad (26)$$

For monoliths of identical composition, this ratio reduces to

$$\mathcal{R}_{monolith} = \frac{19 R_p Q_s}{28 R_s Q_p}. \quad (27)$$

Thus for $Q_s/Q_p = 1$,⁴ eccentricity damping would require $R_p/R_s < 1.47$ corresponding to a mass ratio less than 3.20. For primary and secondary composed of spherical elements with identical compositions and Q 's, the ratio reads

$$\mathcal{R}_{spheres} = \frac{19}{28} \left(\frac{R_p}{R_s} \right)^{1/3}, \quad (28)$$

⁴Identical compositions do not guarantee identical Q_s , because the latter may also depend on strain, strain rate, temperature, and pressure.

so eccentricity would damp for $R_p/R_s < 3.2$ corresponding to a mass ratio below 33. Finally, for rubble piles composed of irregular elements of identical compositions and Q 's,

$$\mathcal{R}_{rubble} = \frac{19}{28} \quad (29)$$

so eccentricity would damp for all mass ratios.

It is clear that eccentricity damping is more likely for binary rubble piles than for binary monoliths especially when the mass ratio is not large. However, given the uncertainties in the relative values of the primary's and secondary's $\tilde{\mu}_{rubble}$ and Q , eccentricity growth remains a possibility, in particular for large mass ratios.

This research was supported in part by an NSF grant and a NASA grant. RS is an Alfred P. Sloan Fellow, and a Packard Fellow. We thank Hiroo Kanamori for valuable advice.

REFERENCES

- Duffy, J., & Mindlin, R. D. 1957, *Journal of Applied Mechanics*, 24, 585
- Gladman, B., Michel, P., & Froeschlé, C. 2000, *Icarus*, 146, 176
- Goddard, J. D. 1990, *Proceedings: Mathematical and Physical Sciences*, 430, 105
- Goldreich, P. 1963, *MNRAS*, 126, 257
- Goldreich, P., & Soter, S. 1966, *Icarus*, 5, 375
- Jacobson, R. A., & French, R. G. 2004, *Icarus*, 172, 382
- Lowry, S. C., Fitzsimmons, A., Pravec, P., Vokrouhlický, D., Boehnhardt, H., Taylor, P. A., Margot, J.-L., Galád, A., Irwin, M., Irwin, J., & Kusnirák, P. 2007, *Science*, 316, 272
- Margot, J. L., & Brown, M. E. 2003, *Science*, 300, 1939
- Murray, C. D., & Dermott, S. F. 2000, *Solar System Dynamics* (Solar System Dynamics, by C.D. Murray and S.F. Dermott. ISBN 0521575974. <http://www.cambridge.org/us/catalogue/catalogue.asp?isbn=0521575974>. Cambridge, UK: Cambridge University Press, 2000.)
- Ostro, S. J., Margot, J.-L., Benner, L. A. M., Giorgini, J. D., Scheeres, D. J., Fahnestock, E. G., Broschart, S. B., Bellerose, J., Nolan, M. C., Magri, C., Pravec, P., Scheirich, P., Rose, R., Jurgens, R. F., De Jong, E. M., & Suzuki, S. 2006, *Science*, 314, 1276

- Porco, C. C., Thomas, P. C., W., W. J., & Richardson, D. C. 2007, *Science*, in press
- Taylor, P. A., Margot, J.-L., Vokrouhlický, D., Scheeres, D. J., Pravec, P., Lowry, S. C., Fitzsimmons, A., Nolan, M. C., Ostro, S. J., Benner, L. A. M., Giorgini, J. D., & Magri, C. 2007, *Science*, 316, 274
- Veverka, J., Thomas, P., Harch, A., Clark, B., Bell, III, J. F., Carcich, B., Joseph, J., Chapman, C., Merline, W., Robinson, M., Malin, M., McFadden, L. A., Murchie, S., Hawkins, III, S. E., Farquhar, R., Izenberg, N., & Cheng, A. 1997, *Science*, 278, 2109
- Walsh, K. J., & Richardson, D. C. 2006a, *Icarus*, 180, 201
- Walsh, K. J., & Richardson, D. C. 2006b, in *Bulletin of the American Astronomical Society*, Vol. 38, *Bulletin of the American Astronomical Society*, 582–+
- Yeomans, D. K., Barriot, J.-P., Dunham, D. W., Farquhar, R. W., Giorgini, J. D., Helfrich, C. E., Konopliv, A. S., McAdams, J. V., Miller, J. K., Owen, Jr., W. M., Scheeres, D. J., Synnott, S. P., & Williams, B. G. 1997, *Science*, 278, 2106

Asteroid name	Orbital period (days)	Semimajor axis (km)	Primary diameter (km)	Secondary diameter (km)	Monolith age (Gyr)	Fluid age (yr)	Rubble Pile age (Myr)
(66391) 1999 KW ₄	0.73	2.5	1.2	0.4	15	37	7.5
1999 HF ₁	0.58	7.0	3.5	0.8	3.6	74	5.2
(5381) Sekhmet	0.52	1.5	1.0	0.3	4.2	7.0	1.7
(66063) 1998 RO ₁	0.6	1.4	0.8	0.38	4.1	4.4	1.3
1996 FG ₃	0.67	2.6	1.5	0.47	4.3	16	2.7
(88710) 2001 SL ₉	0.68	1.4	0.8	0.22	24	26	7.8
1994 AW ₁	0.93	2.3	1	0.5	14	23	5.6
2003 YT ₁	1.2	2.7	1	0.18	880	1500	360
(35107) 1991 VH	1.4	3.2	1.2	0.44	74	180	36
2000 DP ₁₀₇	1.8	2.6	0.8	0.3	540	580	180
(65803) Didymos	0.49	1.1	0.8	0.17	11	12	3.7
(5407) 1992 AX	0.56	6.8	3.9	0.78	2.1	54	3.4
(85938) 1999 DJ ₄	0.74	0.8	0.4	0.17	55	15	9.0
2000 UG ₁₁	0.77	0.4	0.2	0.08	280	18	22
(3671) Dionysus	1.2	3.8	1.5	0.3	190	720	120
2002 CE ₂₆	0.67	5.1	3	0.21	88	1300	110

Table 1: Ages of NEA binaries based on assuming their semimajor axes have evolved from much smaller initial values [eq. (22)]. Comparison for monolithic ($k = 3/2\tilde{\mu}$), fluid ($k = 3/2$), and rubble pile ($k = 3/2\tilde{\mu}_{rubble}$) strength for primary. Binary parameters from compilation by Walsh & Richardson (2006a).